SSC02-VII-7

Series of Satellite Encounters to Solve Autonomous Formation Assembly Problem

Tamas Kormos , Dr. Phil Palmer, Prof. Sir Martin Sweeting

Surrey Space Centre
University of Surrey, Guildford, Surrey, UK
Tel +44 1483 689278, Fax +44 1483 689503
T.Kormos@surrey.ac.uk

Abstract: This paper addresses the problem of bringing two satellites on different orbital planes together and presents results of successful experiment done using two SSTL satellites: UoSat-2 and UoSat-12.A simple linearized Keplerian model with J2 dynamics included was used for initial approximation. A standard LQR controller is presented which by using the above model provides optimal along-track only firing strategy to bring the satellites within a few kilometres of each other. A high precision analytical propagation determines the exact geometry and time of closest approach. As the inclinations of the above two satellites differ by more than 30 degrees, the final step of bringing the two satellites into a stable formation was obviously left out, but radio receiver data from the fly-by are presented to validate the accuracy of the method. A nonlinear least squares filter was constructed to extract orbital elements from the radio data received, thus improving our knowledge of the relative orbits of the two satellites. We have brought the two satellites at closest 7.7 km, while other encounters happened at much larger distances. Clear radio signals were received when the satellites were even 150 km apart. For selected encounters for which we have good quality radio data, we were able to confirm that our prediction was 0.451 second accurate with respect timing and 2.29 km with respect closest approach distance (rms).

Introduction

Formation assembly targets the problem of bringing satellites together within a specified proximity of each other. This is needed, as after separation from the launcher, members of the formation could potentially be on different orbits and drifting apart while the spacecraft are commissioned. Formation assembly also needed when new spacecraft are being launched to join an existing formation. In spite of the recent flurry in formation flying technologies [4-6], literature on formation assembly is rather small, but a field nonetheless which needs more attention.

The spacecraft supplier and operator, Surrey Satellite Technology Limited has built and launched numerous LEO satellites over the past decades, and a goal was established to bring together two of them (UoSat-12 and UoSat-2) together in close proximity of each other. Even though the inclination difference between the orbits of the two spacecraft is more than 30^0, it was proposed to investigate formation assembly scenarios and the possibility of synchronized encounters between the two satellites.

Parameter	Uo-2	Uo-12
semi-m axis (km)	7019.08	7025.41
eccentricity	9.344e-4	2.019e-3
inclination (°)	98.06	64.5774
RAAN (°)	47.17	314.97
arg. of perigee (°)	-152.2	136.39
arg. of latitude (°)	-121.65	-102.77

Table 1: Uo-2 and Uo-12 orbital elements on 20th March 2002, 10:20:00

Analytic Prediction Model

The analytic prediction of the encounter happens in two major steps using the epicyclic[1] description of satellites by Hashida and Palmer. Initially we aim to get the satellites within a few kilometers of each

other and without worrying what is the exact geometry. Thus at this step we do not have to worry about eccentricities of satellites, collision just on which days the satellites are going to be close to each other and what are their phase angles will be at the time of fly-by. However because of the long time scales involved we do have to worry about secular J_2 (second zonal harmonic of the non-spherical geopotential) and aerodynamical drag effects.

In the second step we use analytical propagation to find exact parameters and geometry of the encounter. Once the exact time of the encounter is found a plane-change maneuver could be executed to finalize formation assembly. However in this case it was obviously left out for the angular difference between the two orbit planes would make this impossible.

The epicyclic equations of orbit of a satellite as descried in the first step, ignoring any second order effects and drag for the moment, are:

$$r = a(1 + \mathbf{r}) + b \tag{1}$$

$$\mathbf{l} = n(t - t_E)(1 + \mathbf{k}) - \frac{3b}{2a}n(t - t_E) \tag{2}$$

$$I = I_0 \tag{3}$$

$$\Omega = \Omega_0 + \mathbf{q}(t - t_0) \tag{4}$$

where $r, \mathbf{l}$ describe the motion of the satellite in the instantaneous orbit plane without eccentricity and the J_2 constants are

$$\mathbf{r} = -\frac{1}{4}J_2(R/a)^2(2 - 3\sin^2 I_0) \tag{5}$$

$$\mathbf{k} = \frac{3}{4}J_2(R/a)^2(4 - 5\sin^2 I_0) \tag{6}$$

$$\mathbf{q} = -\frac{3}{2}J_2(R/a)^2\cos(I_0) \tag{7}$$

and a is the guiding centre radius, b is the offset in radial direction, t_E is equator crossing time.

Let us denote satellite 1 (UoSat-2) parameters with subscript 1 and satellite2 (UoSat–12) parameters with subscript 2. We have also the freedom to choose the initial guiding centre of satellite 1 to be at the same radius as it follows from its semi-major axis and thus we have $b_1 = 0$. For our purposes we now denote b_2 simply b, and $a = a_1 = a_2$.

As shown in Figure 1, now we have a spherical triangle, where the two circles of radius $a(1 + \mathbf{r})$ intersect the equator and each other. The intersection point X is defined as encounter point, and if the satellites are phased right the satellites are expected to be within several kilometers of this point (and each other) at the same time.

We also define b and all J_2 terms as being small or first order (10^{-3}) with respect to Keplerian two-body
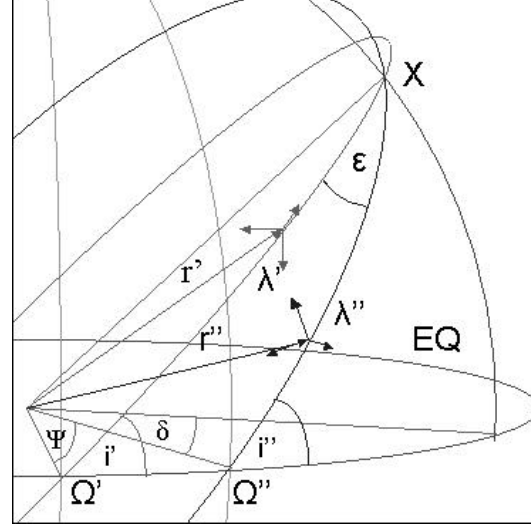
motion. For the first analysis all second order terms will be ignored.

Now from spherical geometry (Figure 1.) we have:

$$\Psi = \Omega_2 - \Omega_1 = \Delta\Omega_0 + n(t - t_0)(\mathbf{q}_2 - \mathbf{q}_1) \tag{8}$$

$$\cot \mathbf{I}_1 = \cot \Psi \cos I_1 - \frac{1}{\sin \Psi}\frac{\sin I_1}{\sin I_2} \tag{9}$$

$$\cot \mathbf{I}_2 = -\cot \Psi \cos I_2 + \frac{1}{\sin \Psi}\frac{\sin I_2}{\sin I_1} \tag{10}$$

Figure 1: Formation assembly geometry in general case

Immediately we can have a rough estimate on the relative velocities of the satellites, or how much delta V we would need for an immediate plane change maneuver by calculating the angle ε.

$$\cos \mathbf{e} = -\cot \mathbf{I}_1 \cot \mathbf{I}_2 + \frac{\cos \Psi}{\sin \mathbf{I}_1 \sin \mathbf{I}_2} \tag{11}$$

This is because ignoring eccentricities allow us to say that the angle between the velocity vectors of the satellites at point X is ε.

If satellite 1 has crossed the equator at time t_{E1} and its guiding center is at X at time t_1, then we have:

$$\mathbf{l}_1 = n(t_1 - t_{E2})(1 + \mathbf{k}_1) \tag{12a}$$

and similarly for satellite 2

$$\mathbf{l}_2 = n(t_2 - t_{E2})(1 + \mathbf{k}_2) - \frac{3}{2}\frac{b}{a}n(t_2 - t_{E2}) \tag{12b}$$

Rearranging to get the time difference between the satellites arriving close to each other while ignoring second order terms:

$$G = t_1 - t_2 = [\frac{\boldsymbol{I}_1}{n}(1 - \boldsymbol{k}_1) - \frac{\boldsymbol{I}_2}{n}(1 - \boldsymbol{k}_2 + \frac{3b}{2a})] \quad (13)$$
$$+ t_{E1} - t_{E2}$$

Thus at any time if satellite 2 is at X, then G gives the time difference of satellite 1 being at X as well. If G=0, then we define encounter between the satellites. To find out when we will have encounter we simply solving for G=0 as time progresses.

We have to bear in mind that the difference between the equator crossing times also progresses every orbit the following way:

$$t_{E1}' = t_{E1} + \frac{2\boldsymbol{p}}{n}(1 - \boldsymbol{k}_1) \quad (14)$$

$$t_{E2}' = t_{E2} + \frac{2\boldsymbol{p}}{n}(1 - \boldsymbol{k}_2 + \frac{3b}{2a}) \quad (15)$$

$$\Delta t_E' = \Delta t_E + \frac{2\boldsymbol{p}}{n}(\boldsymbol{k}_2 - \boldsymbol{k}_1 - \frac{3b}{2a}) \quad (16)$$

from eq 8. we also have

$$\Psi' = \Psi + 2\boldsymbol{p}(\boldsymbol{q}_2 - \boldsymbol{q}_1) \quad (17)$$

and finally substituting 16 into 13

$$G' = G + \frac{2\boldsymbol{p}}{n}[\boldsymbol{I}_1(\Psi)' - \boldsymbol{I}_2(\Psi)']$$
$$(\boldsymbol{q}_2 - \boldsymbol{q}_1) + \frac{2\boldsymbol{p}}{n}(\boldsymbol{k}_2 - \boldsymbol{k}_1 - \frac{3b}{2a}) \quad (18)$$

where $\boldsymbol{I}(\boldsymbol{Y})'$ is derivative with respect to $\boldsymbol{y}$. Using the transformation

$$\boldsymbol{I}_1(\Psi)' - \boldsymbol{I}_2(\Psi)' = \frac{\sin(\boldsymbol{I}_1 - \boldsymbol{I}_2)}{\sin \Psi} \quad (19)$$

the proof of which would be too long to present here, we can establish an optimal separation b_c such that G'=G:

$$b_c = \frac{2a}{3}[(\boldsymbol{k}_2 - \boldsymbol{k}_1) + \frac{\sin(\boldsymbol{I}_1 - \boldsymbol{I}_2)}{\sin \Psi}(\boldsymbol{q}_2 - \boldsymbol{q}_1)] \quad (20)$$

Thus if G=0 and satellite 2 can always maintain its semi-major axis with a separation of b_c from satellite 1, then we would have continuous encounters between the two satellites. In other words we can use drift caused by varying the semi-major axis to counteract drift caused by the J_2 terms and synchronize the phases of satellites so they meet twice every orbit.
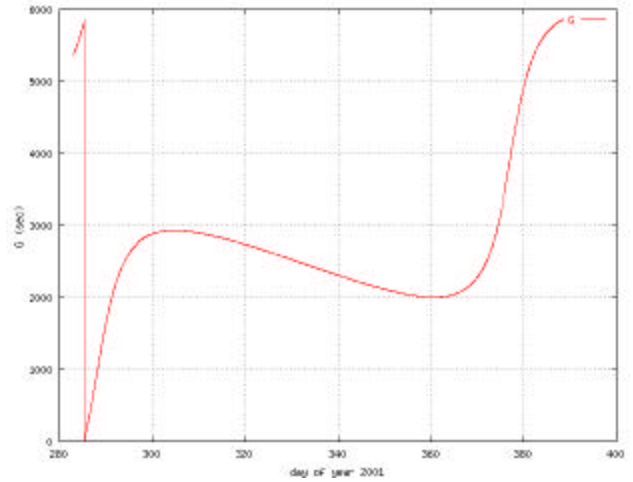

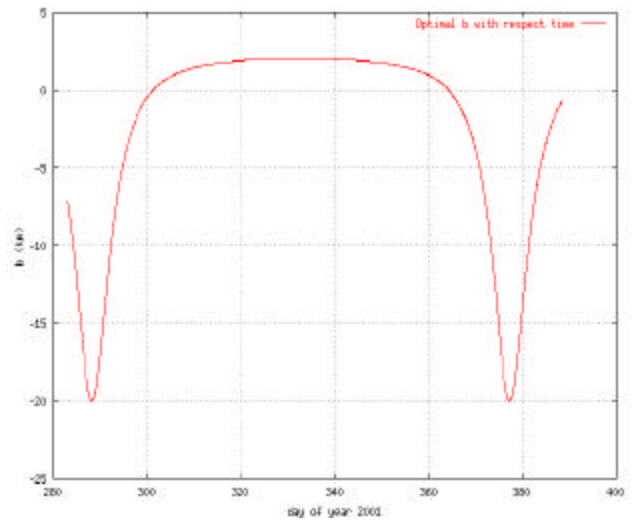**Figure 2**: Function G, with respect time

Figure 3: b_c with respect time

Graphs 2 and 3 show example behavior of the G and b_c functions with respect to time. As mentioned before we have encounter when G=0=2π/n or any integer number of orbital periods. Please note that b_c can vary between +2 and -20 km and that is mainly because of the large difference in the inclinations causing large differential J_2 disturbances.
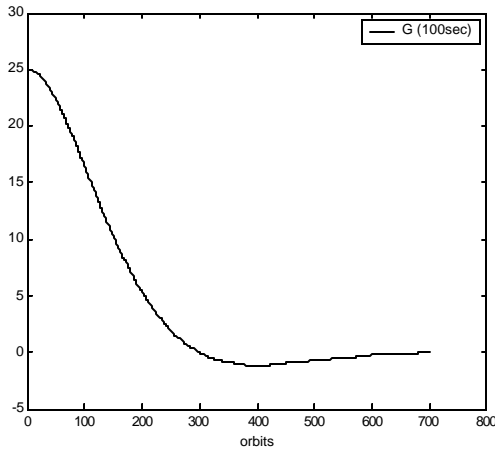
LQR Control and firings

We can now define our LQR problem as to reduce both G and $h=b-b_c$ to zero. Accordingly our state vector contains G and h. Although b_c varies with time, we know its exact value. Thus in our control loop we modify G external to the LQR algorithm to achieve our desired result. Our state transition equation is thus:

$$\begin{pmatrix} G \\ h \end{pmatrix}_{k+1} = \begin{pmatrix} 1 & -\dfrac{3\boldsymbol{p}}{a} \\ 0 & 1 \end{pmatrix} \begin{pmatrix} G \\ h \end{pmatrix}_k + $$
$$\begin{pmatrix} -\dfrac{3\boldsymbol{I}_2}{2an} - \dfrac{3\boldsymbol{p}}{an} \\ 1 \end{pmatrix} \Delta h + \begin{pmatrix} \dfrac{3b_c\boldsymbol{p}}{an} \\ 0 \end{pmatrix} \qquad (21)$$
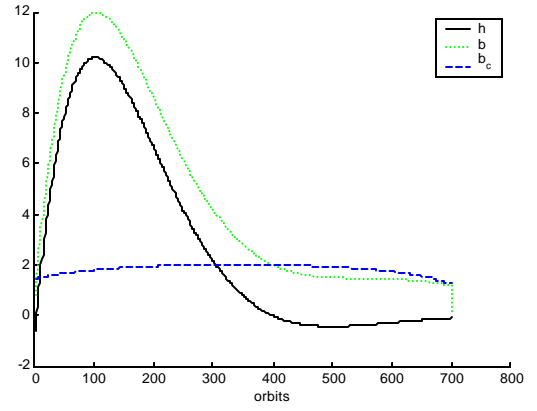
Simulations were done in MATLAB using the DLQR function K=DLQR(A,B,Q,R), where Q=[1 0; 0 0] and R=1e8 and A and B as specified in equation 21. It is imperative to note that coefficients would need to be chosen separately for each scenario to find the required trade-off between time and fuel.

The following figures show a scenario, where the initial value of G is 2500 seconds (almost half an orbit) and it takes the controller approximately 700 orbits of firings to bring the satellites in synchronized formation flying. This somewhat worse case scenario with respect fuel expenditure needs 22 km of semi-major axis change, which is about 11.8 m/s total delta-v. Obviously by waiting while the natural dynamics brings the two satellites closer could significantly reduce this. It is also worthy to note that after G becomes close to 0, maintenance of the synchronized encounters cost less than 1m/s. This is because a period was chosen where the variation of b_c is small.
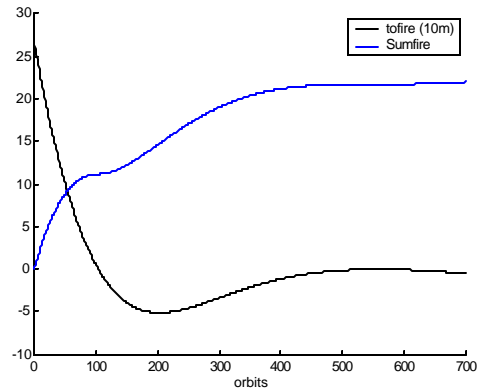
The LQR controller was also verified by replacing the analytical model high-precision numerical propagators [3] and inserting the commanded delta-vs in an open-loop control manner.

Figure 5: Plot of h,b,b_c (km) vs orbits

Figure 6: Plot of to_fire (10m) Sum_fire (km) vs orbits

To simplify our control process relative aerodynamical drag was added at the final stage of the process. After drag coefficients were estimated via the OBC or NORAD, the relative change in b until the next firing period was subtracted from the $b'-b$ value from which the firing command was calculated. This rather simplified approach is justified by the fact that relative drag between the satellites is very small compared to the manoeuvres executed and errors gained via incorrect attitude or not perfectly calibrated propulsion.

In total more than 50 firings were executed on UoSat-12 by firing usually once a day. Another aim for the firings were to reduce the eccentricity of UoSat-12, radial firings were executed as well.

The Table 2 shows some of the firings executed.

Figure 4: Plot of G (100 sec) vs orbits

Date	Direction	SMA-before (km)	SMA-after (km)	SMA-change(km)
21/02/02	Alongtrack+	7026.062	7026.19764	0.1353006
22/02/02	Alongtrack +	7026.199	7026.30777	0.1087635
23/02/02	Radial -	7026.312	7026.30533	-0.006984
24/02/02	Radial -	7026.306	7026.30261	-0.0034
25/02/02	Radial -	7026.303	7026.28793	-0.015153
26/02/02	Radial -	7026.288	7026.26668	-0.021083
27/02/02	Alongtrack -	7026.275	7026.20039	-0.074757

Table 3: 7 of the firings executed on UoSat-12

Collision Analysis

After the initial analytical prediction and firings we used the full epicycle model [2], including the eccentricities this time, to analytical propagate the satellites and predict the final parameters of the encounter. Table 3 shows example output of the final prediction.

Date	Closest approach (km)
20/03/ 2002 09:32:58	25.85991
20/03/ 2002 10:21:44	14.0059
20/03/ 2002 11:10:38	13.33353
20/03/ 2002 11:59:23	16.4301

**Table 4:** Example output of final prediction

However it is different to predict what is happening 2-3 days before the encounter or two weeks before it. Although our accuracies would improve a lot as time progresses, the capabilities to change on the encounter parameters are reduced due to limitations of the propulsion system. On the other hand estimating the exact phases of the satellites two weeks before is rather difficult because of drag.

Thus a simple statistical analysis was used to ensure that the satellites would not get too close. Knowing the inaccuracies of the orbit estimation and our analytical model, 500 random, Gaussian distribution variations were added and propagated to the satellites. The closest approach was extracted each time and the results organized in a histogram.

The fact that for the March the 20th encounter the satellites could get as close as 2 km was a bit threatening. Although the final closest approach was modified because of the collision analysis, the next encounter was set up with the knowledge of how initial conditions can affect the final parameters of the encounter. Thus for April even two weeks before the actual encounter we could be sure that the satellites would not get as close as 13 kilometres.
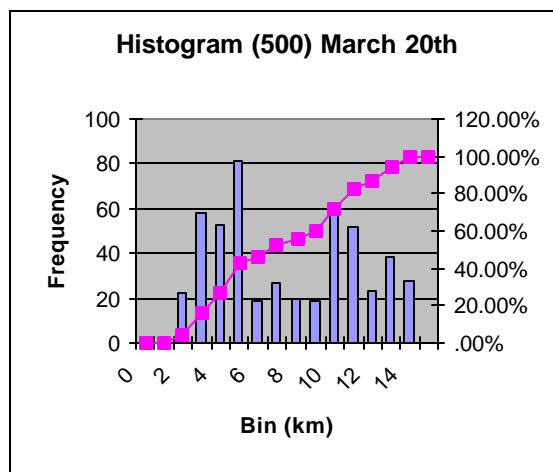
Figure 7: Collision analysis in March
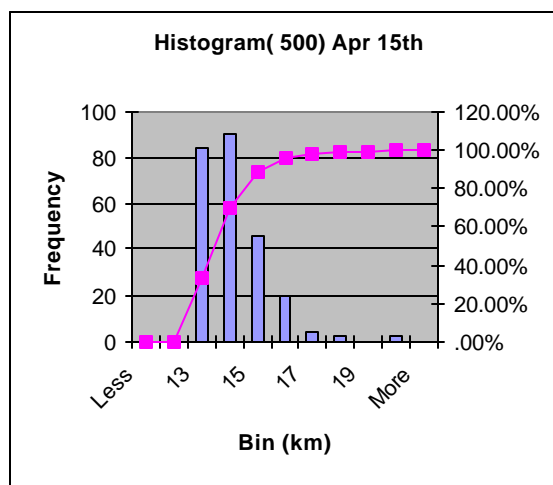
Figure 8: Collision analysis for encounter in April
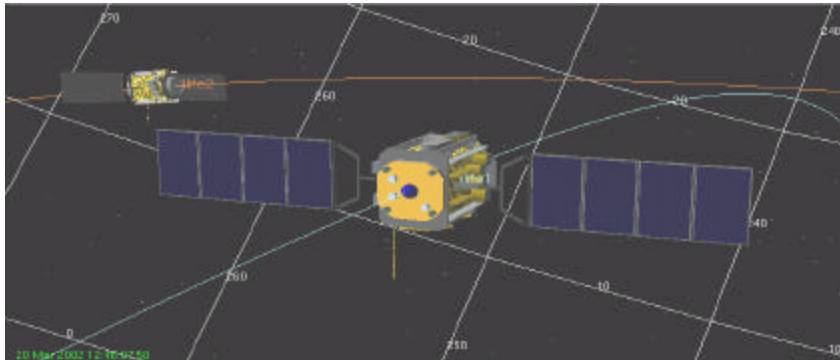
Figure 9: Screenshot of STK simulation
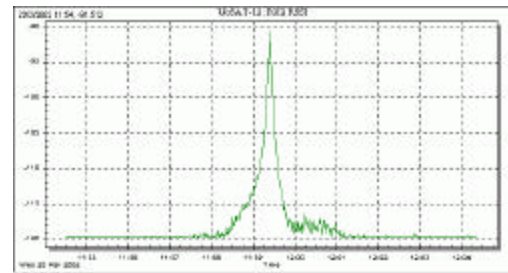showing the orbits crossing

Received Radio Data

There were a total of 26 scheduled encounters for which the radio receiver of UoSat-12 was tuned for the download frequency of UoSat-2. The dates of the encounters were 12th October '01, 20th March and 15th April '02. For the last two cases attitude manoeuvres were executed as well to try to capture images, but without any merit.

This is because the ADCS and the cameras of the SSTL satellites were designed for nadir pointing earth observation goals in mind and not the high accuracy pointing, high slew rates and small integration times needed to take an image of another satellite moving with relative velocities ~10km/s.

On the other hand a clear signal was intercepted from UoSat-2 at all times during the scheduled times. Figures 10-13 show two sets of signal strength and discriminator output. Two things can be immediately deducted from these graphs. First of all the centred nature of the major feature shows that the timing of the window for the encounters was rather good. This was also verified with quantitative methods in the next section.

Secondly we can see that the first data set is much less noisier than the second one. Looking at the actual positions of the satellites during the encounter could explain this, as the second set was taken over populated areas of Sweden, while the first one was taken while the satellites were over unpopulated areas of the pacific near New-Zealand.

A similar trend could be noticed with all the other datasets as well. Because the actual instruments are so accurate that the error bars would be barely visible on these graphs, we can therefore deduce that all fluctuations are due to unknown radio sources and antenna characteristics.
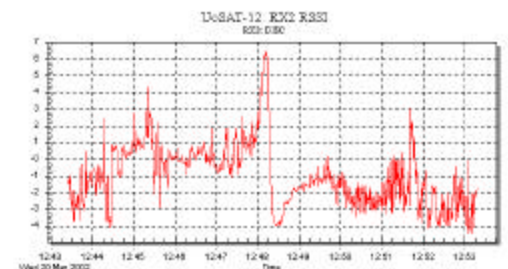

Figure 10: Signal strength over the pacific
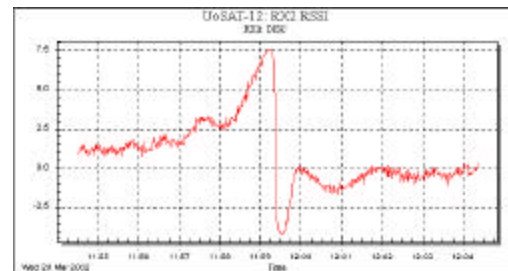
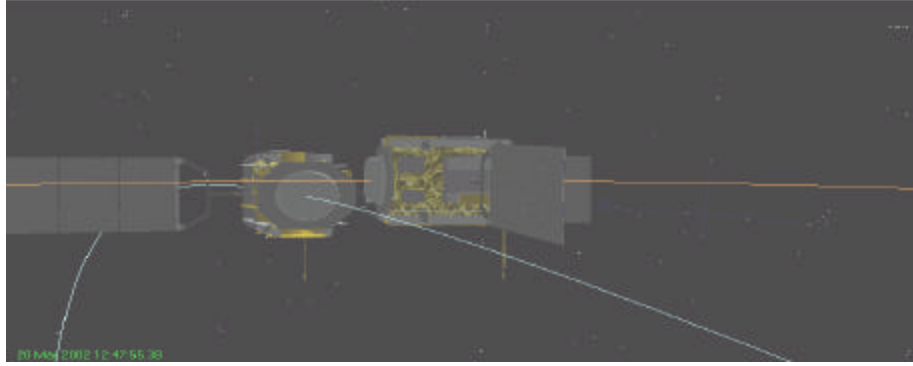**Figure 11**: Discriminator output over pacific
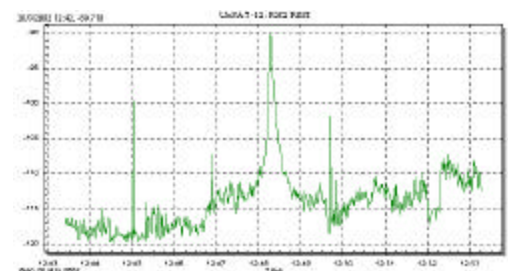
Figure 12: Signal strength over Sweden
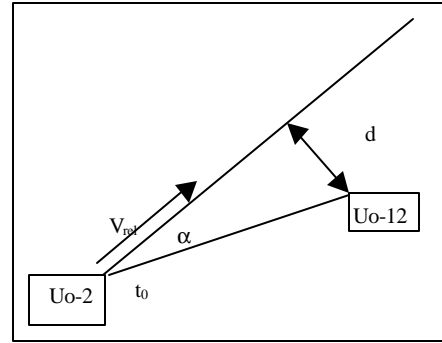

Figure 13: Discriminator output over Sweden

Figure 14: Screenshot of STK simulation showing the orbits crossing

Verification of predictions

After reviewing the datasets, it was found that the Doppler curve of the discriminator output produced a lot more accurate results than the peaks on the signal strength indicator graphs. Further investigation showed that a straight line could, easily approximate the actual relative orbits between UoSat-2 and UoSat-12 during the 15-20 seconds of closest approach. That is looking from the point of UoSat-12, UoSat-2 would be travelling in a straight line with a relative velocity of 10.5 km/s and at the closest approach it would be around 11 km apart. This straight-line fit of the relative orbit segment has got an RMS < 0.5m and thus good enough for our purposes.

For all 26 data sets the middle 20-second part of the discriminator output was extracted. The OBC logged this output every second thus this means 20 data points. The relative velocities between the satellites can be estimated by either the angle ε in equation 11, or via the high accuracy analytical propagation. Into our measurement equation we also had to put in a bias r for there is an about 1.5kHz mis-calibration for the downlink frequency of UoSat-2. The measurement equation is as follows:

$$y(t) = r + \frac{Fout}{c} \frac{v^2(t_0 - t)}{\sqrt{(t_0 - t)^2 + \frac{v^2}{d^2}}} \qquad (22)$$

where F_{out} is the downlink frequency of UoSat-2, c is the speed of light, d is the closest approach distance, v is the relative velocity and t_0 is time at start of filtering.

A standard non-linear least squares [7] algorithm was then used to extract r, d, t_0. However the initial fit was rather poor (Figure 15.) (Table 3). The RMS of the residuals was 0.67.

Figure 15: Straight line approach

	final parameter	standard error	
b (kHz)	1.73126	+/- 0.174	(10.05%)
t0 (sec)	43.1406	+/- 0.09808	(0.2273%)
d (km)	5.84829	+/- 2.242	(38.34%)

**Table 5**: Filter output without velocity correction
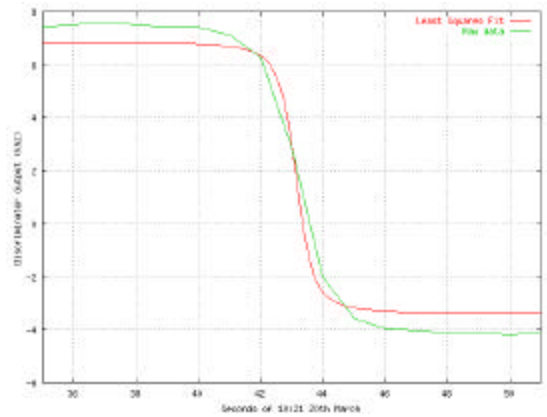
Figure 16: Filter result without velocity correction

It seemed as if the guess for the relative velocity was too low and thus prohibiting a more accurate fit. This was an unknown characteristic of either the discriminator or the antenna of UoSat-12. Thus for the second try we also had to filter for the relative velocity as well. However the actual output of the filter was useless in the sense that it was always 10-15% higher then it is expected thus needed to be discarded. However the quality of the fit has improved significantly (Figure 16.) (Table 4.). The RMS of the residuals in this case was now only 0.06 kHz.

The same filtering procedure was executed for all other datasets and the RMS of the residuals was always less than 0.1 kHz. Summing up all filter outputs we can compare the overall performance in predicting encounter parameters on next day with respect to the received radio data. The RMS error in the timing prediction 0.451 seconds, while the RMS error for closest approach distance was 2.29 km. With respect to the small usable data, the 1 second sampling period and the high relative velocities, it can be concluded that the prediction system worked reasonably well and within the expected error boundaries.

	final parameters	standard error	
b (kHz)	1.68407	+/- 0.0168	(0.9974%)
t0 (sec)	43.206	+/- 0.01061	(0.02455%)
d (km)	11.705	+/- 0.2753	(2.352%)

Table 6: Filter output with velocity correction
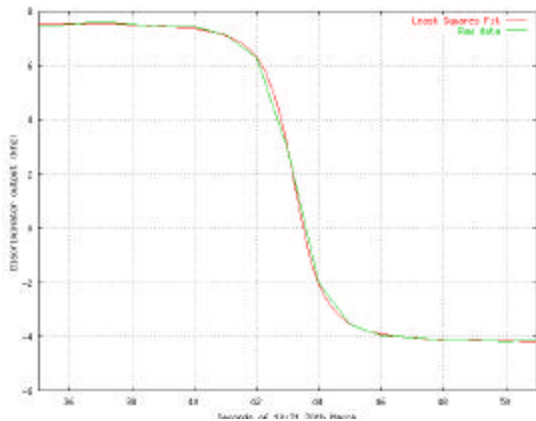
Figure 17: Filter result with velocity correction

Conclusions

In this paper two major topics of formation assembly were discussed. First an analytical model was presented on predicting time of encounters, together with an LQR controller to bring satellites close to each other in a controlled manner. This is achieved by basically counter-acting the drift caused by J_2 terms in the relative phases via changing the semi-major axis of one of the satellites. Sample scenarios showed that control works, but coefficients for the LQR function need to be selected manually.

In the second part real-world experiment results were presented where first part of a formation assembly scenario was executed. Two SSTL satellites were brought in close proximity of each other even though their inclination difference causes a much larger drift then in an ideal formation-flying scenario it is ever possible. Probabilities of collision were examined and on the days of the encounter radio data was received from UoSat-2 via UoSat-12. These 26 real-world data sets were then used to verify the accuracy and the validity of the analytical model developed in the first part.

There are multiple ways to extend on this work. First of all the analytic model could include a full drag model rather than the limited approach used here, to accommodate for scenarios where the drag coefficient between the satellites is rather big.
Secondly a more realistic scenario could be set up by propagating a virtual satellite in an orbit close to UoSat-12's orbit and executing manoeuvres. In this case there would be no risk of collision and the fuel expenditure would be a lot less as well. There fore sustained synchronized encounters and even complete formation assembly could be possible. However the drawback is that there wouldn't be any real world verification like the radio data sets received from UoSat-2 above.

References

1. Hashida ,Y. and P. Palmer, "Epicyclic Motion of Satellites About an Oblate Planet" Journal of Guidance Control, and Dynamics, vol 24, No 3, May-June 2001

2. Hashida, Y and P. Palmer, "Epicyclic Motion of Satellites Under Rotating Potential" Journal of Guidance, Control and Dynamics, Vol 25, No 3, May-June 2002

3. Palmer, P. and S.J. Aarseth and S. Mikkola and Hashida Y. "High Precision Integration Methods for Orbit Modelling" Journal of Astronautical Sciences, Vol. 46, No 4, 1998, pp. 329-342.

4. Koon, W.S. , J.E. Marsden, J. Masdemont, R.M. Murray, "J2 Dynamics and Formation Flight" , AIAA Guidance

Navigation and Control Conference, Aug 2001, Montreal , Canada

5. Hanspeter Schaub, Kyle T. Alfriend, "J2 Invariant Relative Orbits for Spacecraft Formations", NASA GSFC Flight Mechanics and Estimation Conference, 18-20 May 1999, Grenbelt, Maryland

6. Vadali, S.R., S.Vaddi, "Orbit Establishment for Formation Flying of Satellites", AAS/AIAA Space Flight Mechanics Meeting, 23-26 Jan 2000, Clearwater, Florida

7. David A. Vallado "Fundamentals of Astordynamics and Applications", Space Technology Series, McGraw-Hill, 1997

Appendix
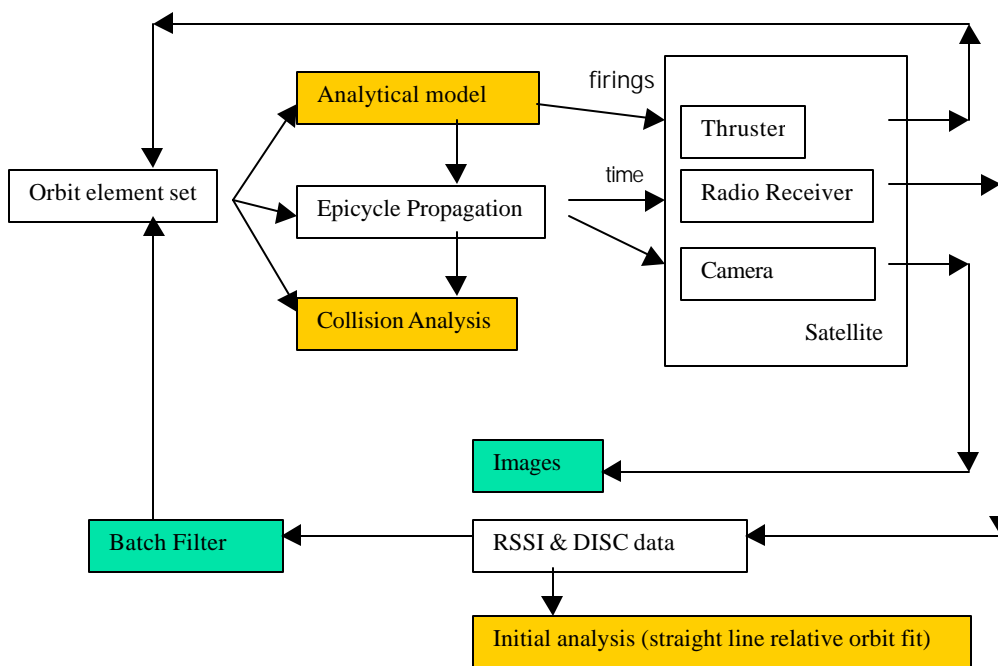
Figure 18: Data flow diagram of the experiment
(RSSI=Receiver Signal Strength Indicator,
DISC=Discriminator Output)